Chapter 3

Migraine mutations impair hippocampal learning despite enhanced long-term potentiation

E. Dilekoz, T. Houben, K. Eikermann-Haerter, M. Balkaya, A.M. Lenselink, M.J. Whalen, S. Spijker, M.D. Ferrari, A.M.J.M. van den Maagdenberg, C. Ayata

J. Neurosci. 35, 3397–402 (2015)

link to Publisher version (online)

Abstract

To explain cognitive and memory difficulties observed in some familial hemiplegic migraine (FHM) patients, we examined hippocampal neurotransmission and plasticity in knock-in mice expressing the FHM type 1 (FHM1) R192Q gain-of function mutation in the CACNA1A gene that encodes the α1A subunit of neuronal $Ca_V2.1$ channels. We determined stimulus intensity–response curves for anterior commissure-evoked hippocampal CA1 field potentials in strata pyramidale and radiatum and assessed neuroplasticity by inducing long-term potentiation (LTP) and long-term depression (LTD) in anesthetized mice in vivo. We also studied learning and memory using contextual fear-conditioning, Morris water maze, and novel object recognition tests. Hippocampal field potentials were significantly enhanced in R192Q mice compared with wild-type controls. Stimulus intensity–response curves were shifted to the left and displayed larger maxima in the mutants. LTP was augmented by twofold in R192Q mice, whereas LTD was unchanged compared with wild-type mice. R192Q mice showed significant spatial memory deficits in contextual fear-conditioning and Morris water maze tests compared with wild-type controls. Novel object recognition was not impaired in R192Q mice; however, mice carrying the more severe S218L CACNA1A mutation showed marked deficits in this test, suggesting a genotype–phenotype relationship. Thus, whereas FHM1 gain-of-function mutations enhance hippocampal excitatory transmission and LTP, learning and memory are paradoxically impaired, providing a possible explanation for cognitive changes detected in FHM. Data suggest that abnormally enhanced plasticity can be as detrimental to efficient learning as reduced plasticity and highlight how genetically enhanced neuronal excitability may impact cognitive function.

Introduction

Familial hemiplegic migraine (FHM) is a monogenic form of migraine with aura, characterized by transient hemiplegia during the aura phase [186]. FHM type 1 (FHM1) is caused by mutations in the *CACNA1A* gene that encodes the pore-forming α_{1A} subunit of $Ca_V2.1$ (P/Q-type) calcium channels [187,188]. Functionally, FHM1 mutations increase $Ca_V2.1$-dependent neuronal Ca^{2+} influx and cortical glutamatergic neurotransmission [110,111,113,189]. As a result, FHM1 transgenic mice display enhanced cortical and subcortical spreading depression susceptibility [110,111,113,190]. Cognitive and memory difficulties have been reported in several families with FHM [191–194] and in small and large cohorts of more common forms of migraine with or without aura [195–197], although not all studies agree on the latter [198]. As one example, standardized neuropsychological tests in a family with six FHM1 patients have shown that although verbal intelligence, verbal memory, and mental arithmetic capacity were normal compared with population averages, specific recall of complex spatial visual cues was markedly impaired [192,193]. Because the latter critically depends on hippocampal, glutamate-mediated neuronal plasticity [199–201], we examined whether such learning deficits are also present in FHM1 transgenic mice and, if so, whether these traits are linked to impaired hippocampal plasticity.

Materials and Methods

Experimental groups

All experiments were performed in accordance with the U.S. Public Health Service Policy on Humane Care and Use of Laboratory Animals and were approved by the Massachusetts General Hospital Subcommittee on Research Animal Care or the animal research committee of the VU University Amsterdam. Female and male FHM1 knock-in mice homozygous for the R192Q mutation or heterozygous or homozygous for the S218L missense mutation [110,111] in the *CACNA1A* gene were compared with wild-type (WT) littermates. Before all experiments, mice were allowed to acclimate for at least 3 days to controlled housing conditions (lights on/off at 7:00 A.M./7:00 P.M.). Before fear-conditioning training, male mice (9–10 weeks) were individually housed with cage enrichment (nesting material and a PVC tube). In all other tests, female mice of 10–16 weeks were used. All investigators were blinded to the genotype of the mice during data collection and analysis.

General surgical procedures

For the electrophysiological experiments, mice were anesthetized (3% isoflurane in 70% N_2O/30% O_2 for induction, 1.5% isoflurane in 70% N_2O/30% O_2 for surgical procedures, and 1.5% isoflurane in 75% N_2/25% O_2 for field potential recordings), and femoral arteries were catheterized for arterial pressure and blood gas measurements. Mean arterial pressure, pH, pCO_2, and pO_2 did not differ between WT and FHM1 mutant mice (73 ± 1 and 72 ± 1 mmHg, 7.34 ± 0.01 and 7.32 ± 0.01, 38 ± 1 and 41 ± 1 mmHg, 115 ± 6 and 115 ± 3 mmHg, respectively). Mice were then placed in a stereotaxic frame (David Kopf Instruments). Rectal temperature was maintained at 37°C (FHC). Under saline cooling, two cranial windows (1 mm diameter) were drilled over the right hemisphere at the following coordinates from bregma: (1) 0.5 mm anterior and 0.5 mm lateral for stimulation electrode and (2) 1.8 mm posterior and 1.5 mm lateral for recording electrode. The dura was kept intact to minimize trauma.

Hippocampal field potential recordings

A glass micropipette filled with 150 mm NaCl was lowered into the stratum pyramidale (1200 µm below dura) using a hydraulic micromanipulator (MO-10; Narishige). Extracellular potentials were recorded using a differential amplifier (EX-1; Dagan) relative to an Ag/AgCl reference electrode placed subcutaneously in the neck and stored using a data acquisition system for off-line analysis (PowerLab 200; ADInstruments). A bipolar stimulation electrode was gradually advanced at the frontal cranial window at a 45° angle in the sagittal plane. Just before reaching the depth of the anterior hippocampal commissure, electrical stimulation was started at 0.1 Hz, using 100 µA, 100 µs square pulses (A395 Stimulus Isolator; WPI). The stimulation electrode was then advanced in small increments until reproducible evoked responses became apparent, and the positions of recording and stimulation electrodes were optimized to obtain maximal local field potentials. After determining the threshold stimulation current required to evoke a pyramidal population spike (63 ± 10 and 97 ± 23 µA in WT and R192Q, respectively; $P = 0.22$), stimulus intensity–response curves for spike amplitude were obtained by increasing the stimulation current in steps of 0.1× spike threshold until 1.6× spike threshold value was reached and then in steps of 0.2× spike threshold until the maximum spike amplitude was obtained. Next, the recording electrode was lowered into the stratum radiatum, and stimulus intensity–response curves for field EPSP (fEPSP) slopes were obtained by increasing the stimulation current

starting from 0.1× spike threshold in steps of 0.3-fold increments until 1.0× spike threshold value was reached, and then in steps of 0.4-fold increments until the maximum fEPSP slope was reached.

Long-term potentiation

Stimulation intensity was set to 50% of the maximal fEPSP slope in each animal. Baseline responses were recorded for 8 minutes (0.1 Hz, 100 µs pulse duration), and three high-frequency stimulus trains (1 s, 100 Hz, 20 s intertrain interval) were applied at test stimulation intensity. Responses were monitored for another 80 minutes. We could not test long-term potentiation (LTP) in the S218L mutant mice because any conditioning stimulus triggered a spreading depression in this highly susceptible strain.

Long-term depression

In a separate group of mice, stimulation intensity was set to 60% of the maximal fEPSP slope. Baseline responses were recorded for 20 minutes, after which 900 paired pulses (37 µs paired-pulse interval, 0.85 Hz) were applied. Responses were monitored for another 50 minutes.

Behavioral tests

Before testing, mice were handled to habituate to the experimenter. The day of the test, mice were carried to the behavioral room and testing started immediately (fear conditioning) or they were allowed to acclimate for 1 hour before the experiments. Behavioral experiments were performed between 8:00 A.M. and 8:00 P.M. The more severe neurological phenotype of the S218L mutants, including cerebellar ataxia and an increased susceptibility to seizures [111], precluded reliable water maze and fear-conditioning testing; therefore, only novel object recognition was tested in this strain.

Fear conditioning

Contextual training and retrieval were performed in a fear-conditioning system (TSE-Systems) as described previously [29]. In brief, mice were placed in an acrylic glass chamber with a stainless steel grid floor for a period of 3 minutes, subjected to a 2 s foot shock (0.7 mA), and returned to their home cage 30 s later. Contextual memory retrieval on the second day consisted of re-exposure (3 minutes) to the context. Shock response [maximum velocity (V_{max})] and freezing were assessed automatically. Freezing was defined as lack of any movement besides respiration

and heart beat during 2 s intervals, presented as a percentage of the total test time. Mice that displayed baseline freezing >20% were considered outliers and were removed from the analysis (n = 1).

Morris water maze

Highly visible cues were located on the walls of each of the four quadrants in a circular water pool (83 cm diameter, 60 cm deep, 21–25°C). A clear Plexiglas goal platform (10 cm diameter) was positioned 0.5 cm below the water surface and 15 cm from the southwest wall. Testing consisted of three periods: hidden platform training, visible platform test, and probe trial. During hidden platform training, mice were placed in the pool facing the pool wall at four starting positions (north, south, east, and west), in randomized order. Mice were given a maximum of 60 s to find the platform. If the mouse failed to reach the platform, it was placed on the platform for 10 s. The average latency to the goal platform was recorded as the latency for that trial. Animals were trained in this way for five sessions once per day for 5 d. To control for possible differences in visual acuity or sensorimotor function between groups, two subsequent trials were performed on day 4, using a visible platform raised 0.5 cm above the surface of the water. One day later, a probe trial was performed in which the mouse was given 60 s to swim in the pool with the goal platform removed. The time spent in the target quadrant (probe time) was recorded for each mouse.

Novel object recognition

During the first session, mice were placed in a rectangular cage (35 × 20 cm) and exposed to two identical objects for 5 minutes. Mice were then allowed to rest in their home cages for 1 hour, followed by a second session during which mice were exposed to a familiar object from the previous session and a novel object for 5 minutes. The discrimination index was calculated as the ratio between the time spent exploring familiar and novel objects during the second session. Because the R192Q and S218L strains share essentially the same genetic background, they were compared with a single pooled WT group.

Statistics

Data were statistically tested using the *t* test, Mann–Whitney *U* test, Kruskal–Wallis test, or two-way ANOVA for repeated measures where appropriate (GraphPad Prism 6.0; GraphPad Software); $P < 0.05$ was considered statistically significant.

Results

Electrophysiology

Stimulation of the anterior commissure evoked characteristic CA1 field potentials comprising a population spike and wave in stratum pyramidale and a dendritic fEPSP in stratum radiatum in both groups (Figure 1). Stimulus–response curves for population spike amplitudes showed a significant left shift in homozygous R192Q mice compared with WT mice. Maximal spike amplitudes were also larger in the mutants (Figure 1C). Stimulus–response curves for fEPSP slopes in the stratum radiatum tended to be steeper, and maximal fEPSP slopes were larger in R192Q mice compared with WT controls (Figure 1D), presumably reflecting enhanced presynaptic excitatory neurotransmitter release.

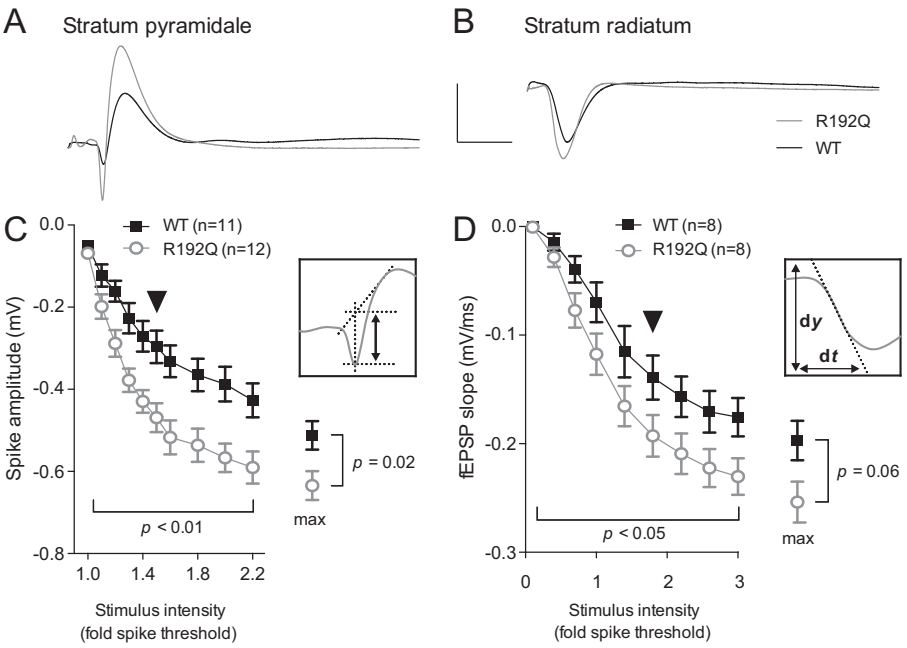

Figure 1: Hippocampal evoked field potentials. Representative responses (**A**; stratum pyramidale, **B**; stratum radiatum; calibration: 0.5 mV, 10 ms) and averaged data show spike amplitude versus stimulus intensity in the stratum pyramidale (**C**) and fEPSP slope in the stratum radiatum (**D**) in WT and R192Q mice. Insets show how spike amplitude (**C**) and fEPSP slope (**D**) were measured. Maximum responses are shown on the right of each curve, obtained at stimulus intensities of 3.7 ± 0.4- and 3.1 ± 0.3-fold spike threshold in stratum pyramidale (**C**) and of 3.9 ± 0.6- and 4.0 ± 0.3-fold spike threshold in stratum radiatum (**D**), in WT and R192Q, respectively ($P > 0.05$). Arrowheads in **C&D** indicate stimulus intensities at which sample tracings in **A** and **B** were obtained. (**C**) The spike amplitude was decreased more in R192Q mutants compared with control (two-way repeated-measures ANOVA, interaction factors stimulus intensity × genotype, $F_{(9,189)} = 3.202$, $P < 0.01$). (**D**) Mutants also showed decreased fEPSP slopes after increased stimulus intensity (two-way repeated-measures ANOVA, interaction factors stimulus intensity × genotype, $F_{(8,120)} = 2.103$, $P < 0.05$). Maximum responses were analyzed using a Student's *t* test. Data are mean ± SE.

High-frequency stimulus trains to induce LTP significantly increased fEPSP slopes in both WT and homozygous R192Q mice (two-way repeated measures ANOVA, factor time, $F_{(167,2338)} = 3.246$, $P < 0.01$), which persisted for at least 60 minutes (Figure 2A,C). LTP magnitude was significantly larger in the FHM1 mutant. Low-frequency paired pulses induced lasting long-term depression (LTD) of fEPSP slopes in both groups (Figure 2B,D; two-way repeated measures ANOVA, factor time, $F_{(193,2316)} = 14.24$, $P < 0.01$). In contrast to LTP, LTD magnitude was identical in WT and homozygous R192Q mice.

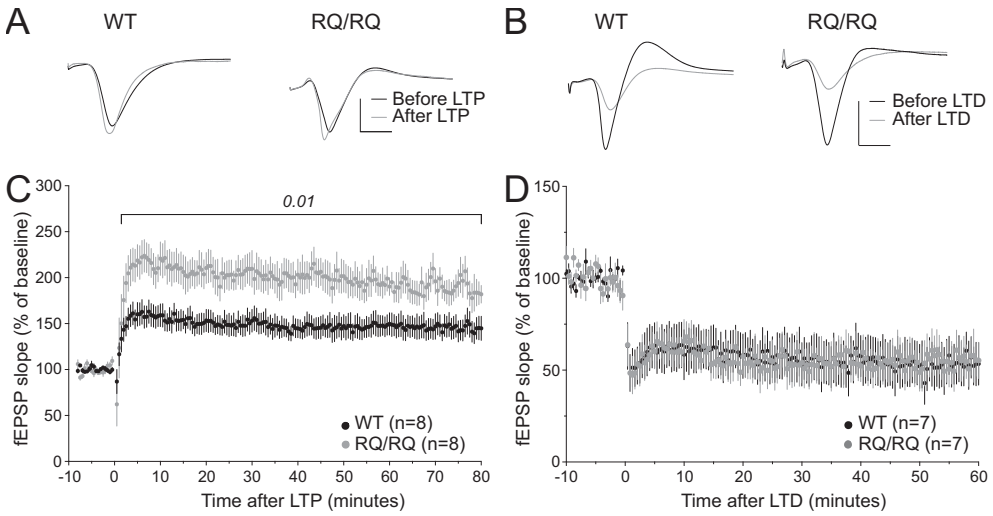

Figure 2: Long-term potentiation and depression in stratum radiatum. (**A**) Representative sweeps show fEPSPs before and after tetanic stimulation to induce LTP (calibration: 0.3 mV, 5 ms). (**C**) After high-frequency stimulation (time 0), the fEPSP slope increased by 1.5-fold of baseline in WT mice and by more than twofold in R192Q mutants (two-way repeated-measures ANOVA starting at 1 minute after stimulation, factor genotype, $F_{(1,14)} = 7.788$, $P = 0.01$). (**B**) Representative sweeps show fEPSPs before and after low-frequency paired-pulse stimulation to induce LTD (calibration: 0.2 mV, 5 ms). (**D**) After low-frequency paired-pulse stimulation (time 0), the fEPSP slope decreased to ~50% of baseline in both WT and R192Q knock-in mice (two-way repeated-measures ANOVA starting at 1 minute after stimulation, factor genotype, $F_{(1,12)} = 0.001$, $P = 0.98$). Data are mean ± SE.

Behavioral testing

We examined WT and FHM1 mice using two learning and memory paradigms that critically depend on hippocampal function [fear conditioning [202], water maze [6]] and a third paradigm believed to rely on distributed connections among multiple brain regions [novel object recognition [203]].

In the contextual fear-conditioning test, mice learn to associate a distinctive context with the unconditioned aversive stimulus, and retrieval of context memory is assessed 24 h later (Figure 3A). Basal freezing time did not differ between WT and mutant strains before shock exposure (Figure 3B). Twenty-four hours later, R192Q mice showed significantly shorter contextual freezing (Figure 3B; Mann–Whitney U test, genotype, $P < 0.01$), indicating impaired contextual hippocampal learning. Importantly, the Vmax response to the 2 s, 0.7 mA shock did not differ between groups, suggesting that mice from both genotypes perceived the shock similarly (Figure 3C).

In the Morris water maze, the time to reach the hidden platform was equal between WT and homozygous R192Q mice during the first training session (Figure 3D, trial 1) and gradually became shorter after repeated sessions in both groups (two-way repeated-measures ANOVA, factor time, $F_{(4,32)} = 7.657$, $P < 0.01$). However, the rate of decrease in time to reach the hidden platform was significantly slower in R192Q mice compared with WT mice, again suggesting impaired spatial learning in FHM1 mice (Figure 3D). Indeed, when mice were reintroduced in the water maze in the absence of the platform (i.e., probe test), R192Q mice spent significantly less time in the quadrant where the platform used to be (Figure 3E). Both groups reached the visible platform at the same time (Figure 3F), suggesting that visual and motor function were comparable between the groups.

In the novel object recognition test, the time spent exploring a novel object compared with a familiar object was similar between WT and R192Q mice. In contrast, both heterozygous and homozygous S218L mice performed significantly worse than the WT mice (Figure 3G; Kruskal–Wallis test followed by Dunn's multiple comparisons test, $P < 0.01$), and homozygous S218L performed significantly worse than R192Q mice (Kruskal–Wallis test followed by Dunn's multiple comparisons test, $P < 0.05$).

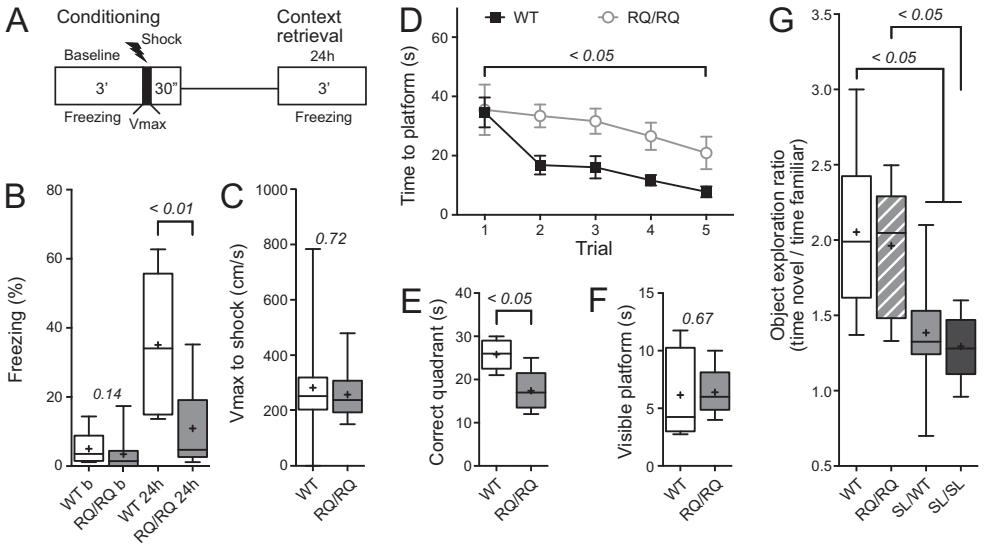

Figure 3: Learning and memory tests. (**A–C**) Fear-conditioning (n = 15 WT/WT, n = 14 RQ/RQ). (**A**) Experimental design for contextual fear conditioning, in which mice were exposed to the context in which they received a shock (2 s, 0.7 mA) after 3 minutes (conditioning) and were re-exposed to the context 24 h later. Readouts include the freezing time and V_{max}. (**B**) Freezing response as percentage of total time spent in the cage in WT (n = 15) and homozygous R192Q (n = 14) knock-in mice at baseline (b) and 24 h later showed a genotype effect for retrieval (Mann–Whitney *U* tests). (**C**) Both groups had a similar reaction to the shock (maximal velocity; V_{max}; Mann–Whitney *U* test), ruling out hypersensitivity or hyposensitivity as a confounder. (**D-F**) Morris water maze (n = 5 WT/WT, n = 5 RQ/RQ). (**D**) FHM1 mice needed more time to reach the hidden platform throughout the 5-day testing period, suggesting impaired spatial hippocampal learning (two-way repeated-measures ANOVA, factor genotype, $F_{(1,8)} = 8.434$, $P < 0.05$). (**E**) Morris water maze probe test. After removal of the platform at the end of training, R192Q mice spent significantly less time in the quadrant where the platform was located (Mann–Whitney *U* test). (**F**) Visible platform test. R192Q mice reached the visible platform at the same time as WT mice (Mann–Whitney *U* test). (**G**) Novel object recognition (n = 15 WT/WT, n = 7 RQ/RQ, n = 10 SL/WT, n = 7 SL/SL). The ratio of time spent exploring a novel object versus a familiar object was comparable in R192Q mice and WT mice but lower in heterozygous and homozygous S218L compared with WT mice. Homozygous S218L mice also performed significantly worse than R192Q mice (Kruskal–Wallis and Dunn's multiple comparisons test). Whisker-box plots show median (horizontal line), mean (+), 25–75% range (box), and full range (whisker). The line graph shows mean ± SE. *P*-values indicated in italic.

Discussion

Our data show for the first time hippocampal network hyperexcitability and its cognitive consequences in a mouse model of FHM1 *in vivo*. Monosynaptic hippocampal CA1 fEPSP slopes were steeper in the stratum radiatum and population spikes larger in the stratum pyramidale, suggesting enhanced glutamatergic neurotransmission and synchronous action potential firing in response to an afferent fiber volley. The LTP of evoked field potentials was significantly stronger in the FHM1 transgenic mice, without a change in LTD. Paradoxically, however, learning and memory in FHM1 mutants was impaired. Memory dysfunction involved paradigms critically dependent on hippocampal function, as well as one that relies on distributed involvement of multiple brain regions, consistent with the complex clinical phenotype.

In most studies, learning and memory changes in the same direction with LTP. The majority of animal models with enhanced LTP shows enhanced learning and memory [61,201,204], and vice versa [199,205]. However, exceptions exist where an inverse relationship between LTP and learning and memory was observed [206–208], resembling our findings in FHM1 mutants. Impaired learning and memory in the presence of overly enhanced LTP is not necessarily counterintuitive [209]. Proper encoding and consolidation of memory, as well as memory recall and subsequent reconsolidation [29], likely requires just the right amount of plasticity. Metaphorically, a completely white page is as uninformative as a completely black page. Too much plasticity would strengthen and perhaps saturate all synapses and be as detrimental to acquisition and recall of memory as is too little plasticity.

It should be noted, however, that although the explanation above is highly plausible, we have not directly recorded hippocampal plasticity during learning tasks and therefore cannot fully substantiate a causal link between enhanced LTP and impaired learning in the mutants. For example, FHM1 mice may develop spontaneous spreading depressions that, if frequent enough, can lead to impaired memory acquisition and recall, much like that observed in transient global amnesia [210,211]. As such, enhanced LTP may not be causally related to impaired memory.

Interestingly, LTD, which also depends on glutamatergic neurotransmission [212], was not augmented in FHM1 mice. In contrast to LTP, however, hippocampal LTD propensity varies depending on the experimental paradigm [213,214], suggesting the possibility that in a different LTD paradigm, FHM1 mutations may augment LTD. Nevertheless, one could speculate that, should there be enhanced LTD, it might

have balanced the enhanced LTP and ameliorated the memory deficits. As such, the combination of enhanced LTP with unchanged LTD may be critical for impaired memory.

The novel object recognition test revealed a critical genotype–phenotype relationship in FHM1 mutants. In contrast to the hippocampus-dependent fear-conditioning and water maze tests, the R192Q mice showed normal novel object recognition, which relies on a more distributed network of brain structures [215]. Only the S218L mutants showed significant deficits in the latter test. It is well established that the R192Q mutation causes weaker $Ca_V2.1$ gain-of-function and a milder (i.e., pure) FHM phenotype than the S218L mutation, both in patients [117,118] and in transgenic mice [110,111,216]. This genotype–phenotype relationship suggests that hippocampal learning and memory is more sensitive to the disruptive effects of FHM1 mutations, whereas an impairment in more distributed learning and memory may require more pronounced changes in glutamatergic neurotransmission caused by the S218L mutation [105,111]. This is reminiscent of the overt ataxia phenotype associated with the S218L but not the R192Q mutation in patients and transgenic mice [111,118].

In summary, the data suggest that a genetic predisposition for enhanced synaptic transmission and spreading depression susceptibility may impact cognitive performance, despite compensatory mechanisms trying to harness the glutamatergic transmission, such as upregulation of glutamate transporters [217].